Supplemental Figures:

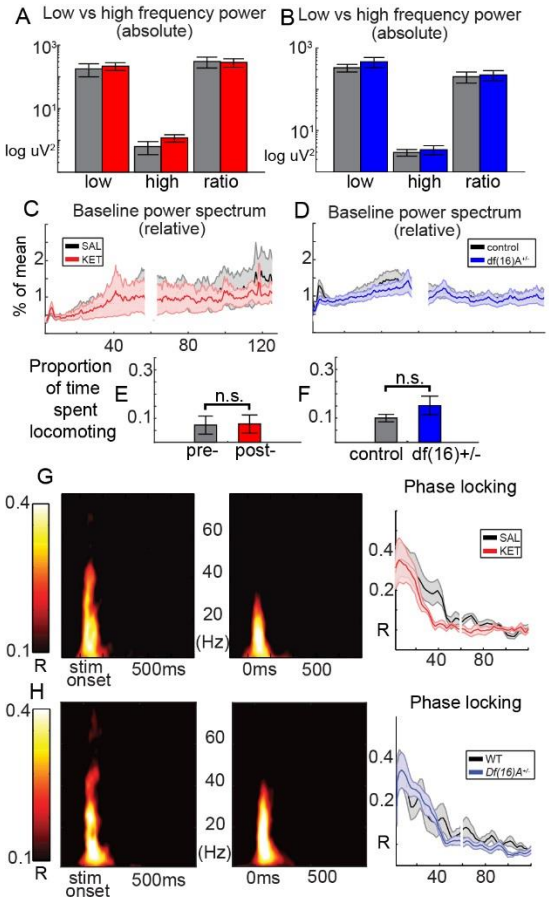

Figure S1. (refers to Figure 1). Indices of arousal and LFP phase dynamics. (**A-B**) Relative to control mice, KET and Df(16)$A^{+/-}$ mice showed a similar ratios of low (<1-15Hz) to high frequency (35-115Hz) absolute power at baseline ($t^{KET}(11)$=-0.14, p=.89; $t^{Df16}(11)$=-0.25, p=.81), and (**C-D**) normalized, or "relative", power spectra (spectrum divided by sum of spectrum within mouse, then adjusted for 1/f component for display) evidence generally similar distributions of power between low and high bands (Harris and Thiele, 2011; Vinck et al., 2015). (**E-F**) KET ($t^{KET}(11)$= t=-0.12; p<0.90; two-tailed) and *Df(16)*$A^{+/-}$ mice (t^{Df16}((11)=-1.35p<0.20; two-tailed) did not differ in the proportion of frames involving locomotion, altogether indicating a lack of gross differences in arousal. Interestingly, *Df(16)*$A^{+/-}$ showed a reduction in relative power limited to the theta peak. **(G-H)** Phase locking of oscillatory activity to the onset of visual stimuli is a commonly computed measure of the consistency of the LFP/EEG response across repetitions of the same type of stimulus, and has been shown to be reduced in schizophrenia (Hamm et al., 2011; Spencer et al., 2004). Results here confirm a reduction in gamma2 for both KET ($t(11)$= 2.33, p<.05) and *Df(16)*$A^{+/-}$ mice ($t(11)$= 3.85, p<.001) and a trend-level decrease in gamma1 for KET ($t(11)$= 1.69, p=.06) and *Df(16)*$A^{+/-}$ mice ($t(11)$= 1.08, p=.15; all spectra/barplots averaged over all mice; n^{sal}=7, n^{ket}=7, n^{df16}=8, $n^{control}$=5; Error bars reflect S.E.M across mice).

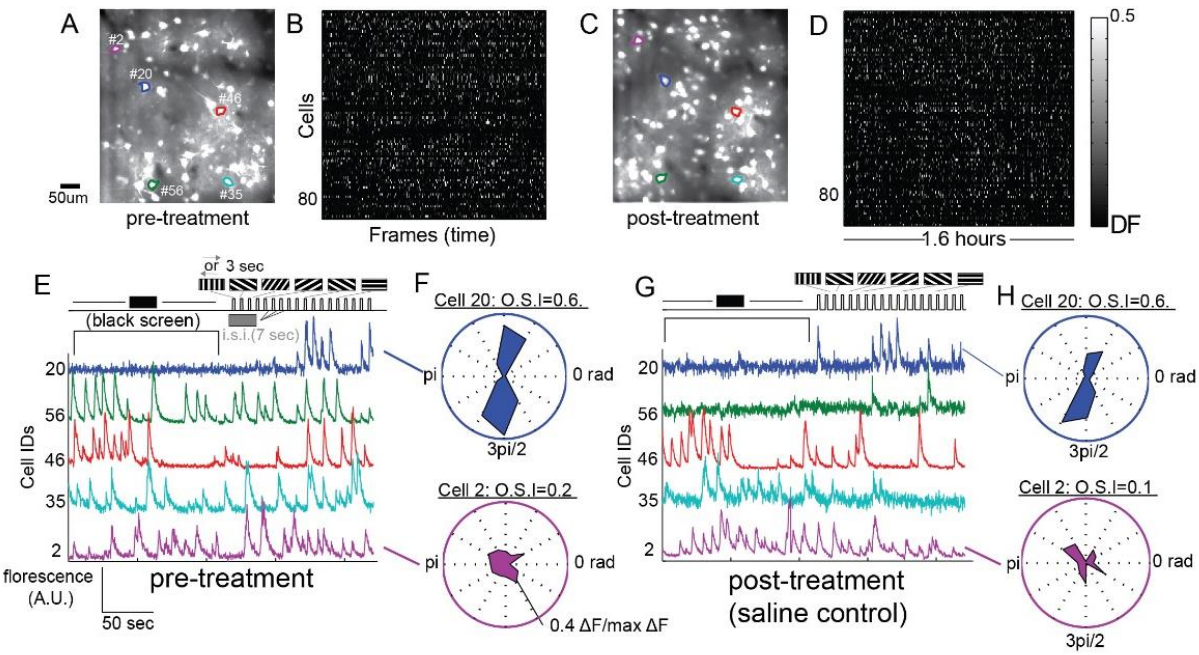

Figure S2. (Refers to figure 2). **Experimental and analytical overview** (**A**) Layer 2/3 of primary visual cortex was infected with an AAV1 to drive expression of florescent calcium indicators GCaMP6s/f in neurons. Florescence was monitored across a 500 by 500 micrometer field of view 200-300 micrometers beneath the surface, and (**B**) individual cells activity was quantified as change in florescence before and (**C-D**) 1 week after implantation of subcutaneous minipump. (**E**) Cell florescence was monitored during a dark-room "rest" period (scored as "ongoing" activity) or during presentation of 3-second moving squarewave gratings (full-field, 100% contrast). (**F**). Cell responses were analyzed as a function of stimulus orientation (O.S.I) or direction (D.S.I, not shown), with average responses within a stimulus type (direction) polar plotted. Panels **G-H** reflect these measurements in the same cells after 1 week of saline.

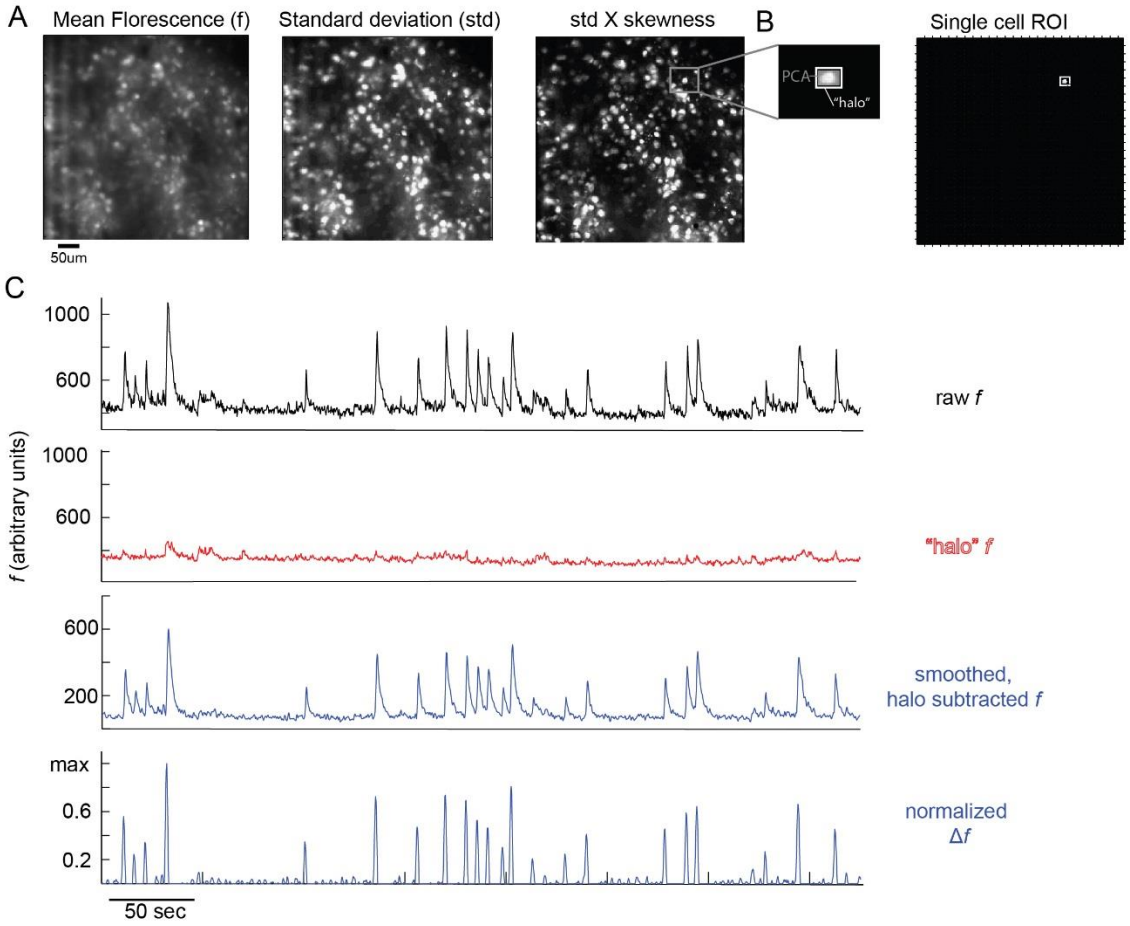

Figure S3. (Refers to figure 2). Data processing and scoring of individual cell activity. (**A**) Pixelwise projections were used to manually identify pixels marking cell bodies, including a mean across frames projection, a standard devaiation across frames projection, and a standard-deviation multiplied by skewness projection (since pixels capturing sparsely active neurons with a minority of active frames will show a large skewness value). (**B**) Rectangular sections were manually selected around cells, where pixels (i) just outside the rectangle were deemed the "halo" (which was later adjusted to exclude other cell bodies), and (ii) within the rectangle were subject to a principal components analysis (unrotated). The first component (pixels with the top 80% of weights) comprised the cell ROI (visually verified for each cell). (**C**) Florescence was averaged within the ROI (top), halo-subtracted, and smoothed with a 3-second lowess filter. The discrete first derivative (central difference between 3 datapoints) was calculated. Δf was then analyzed on the positive resulting values (pre-vs-post single cell analyses) or normalized by dividing by the maximum in the recording session (population analyses; bottom).

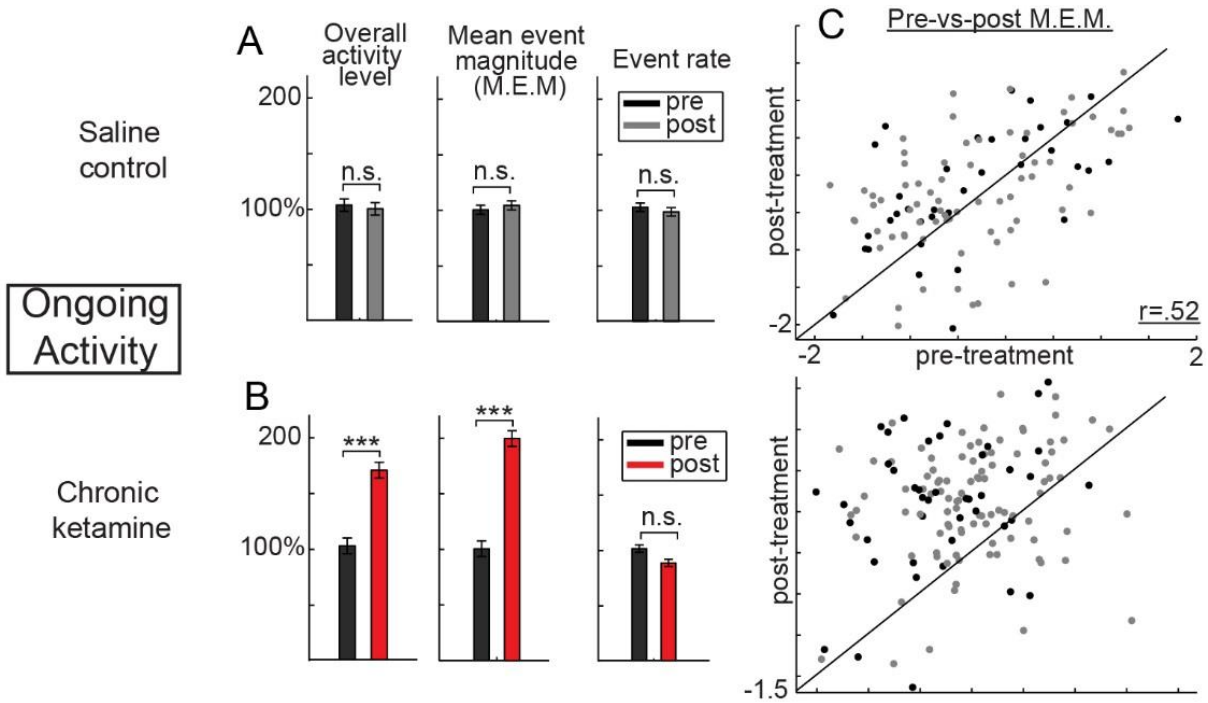

Figure S4. (refers to figure 2). Characteristics and stability of basal calcium activity levels during non-stimulus evoked, ongoing activity. (**A-B**) Overall activity level (proportion of frames with Δf significantly above baseline) and event magnitude (average peak Δ*f* across calcium transient events), but not event rate, were increased in chronic KET. (**C**) pre-vs-post SAL cell activity levels were correlated (p<.01), (**D**) but not KET (r=.22). (n ^{SAL}=117 cells, 4 mice, n ^{KET}=150 cells, 5 mice; Error bars reflect S.E.M across cells). Black dots are visually responsive neurons (O.S.I > .1).

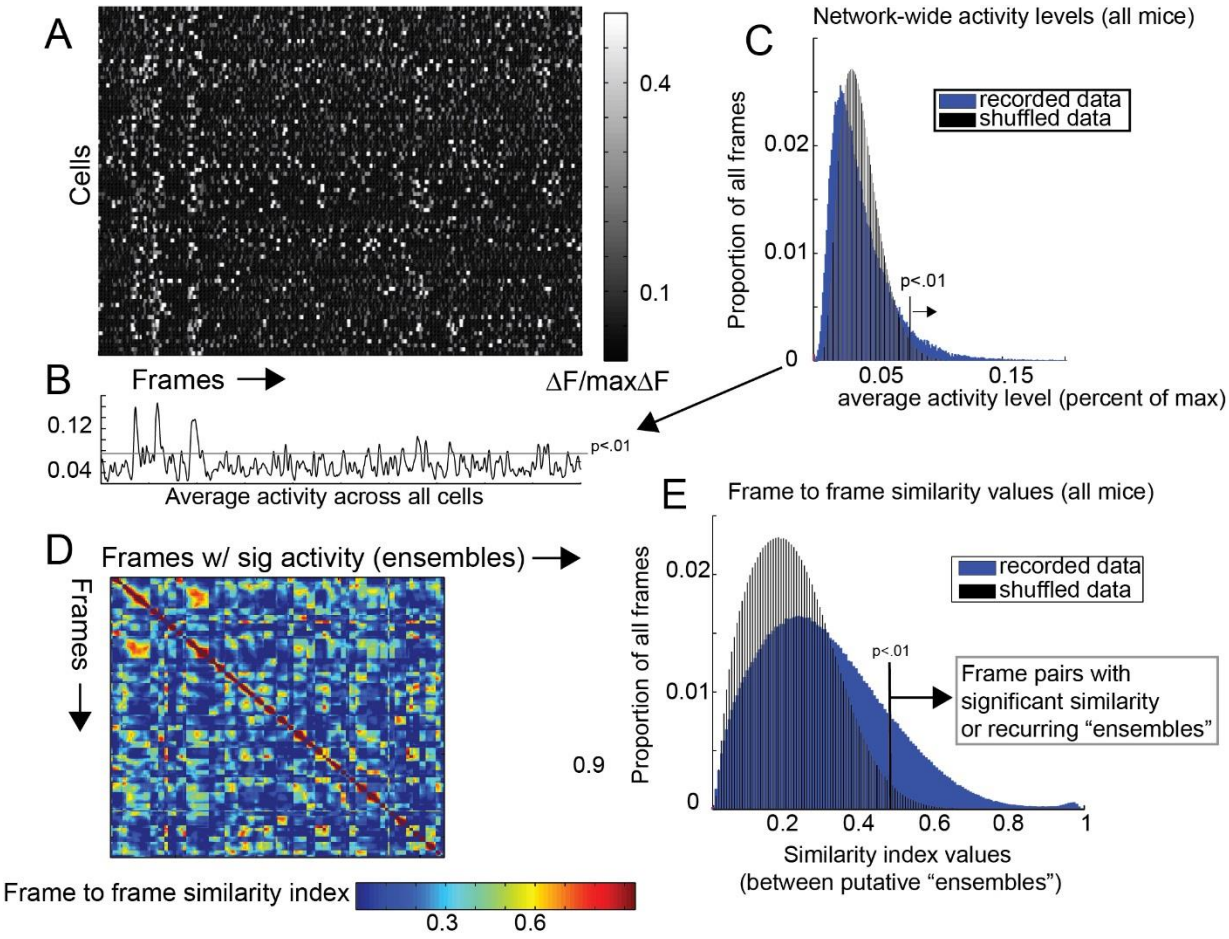

Figure S5. (Refers to figure 3) Statistical assessment of ongoing activity and ensembles. (**A**) Activity across cells (rows) was averaged within frames (columns) to yield (**B**) a network activity time-course for each mouse and treatment. (**C**) Data randomly time-shifted within cells 10000 times determined the 99th percentile for significant coactivity, deemed "ensemble" activations; this value was approximately .06 on average across mice, denoting that ensembles were present when instantaneous activity exceeded at least 6% of the total possible network activity (all cells maximally active at the same time). (**D**) Similarity index, or the magnitude-weighted cosine similarity between activation state n-dimensional vectors (n=number of cells), were calculated between all ensemble frames. (**E**) After shuffling cell activity within frames for all ensembles, 99th percentile for similarity values was determine (S.I.=.45; n=28 mice).

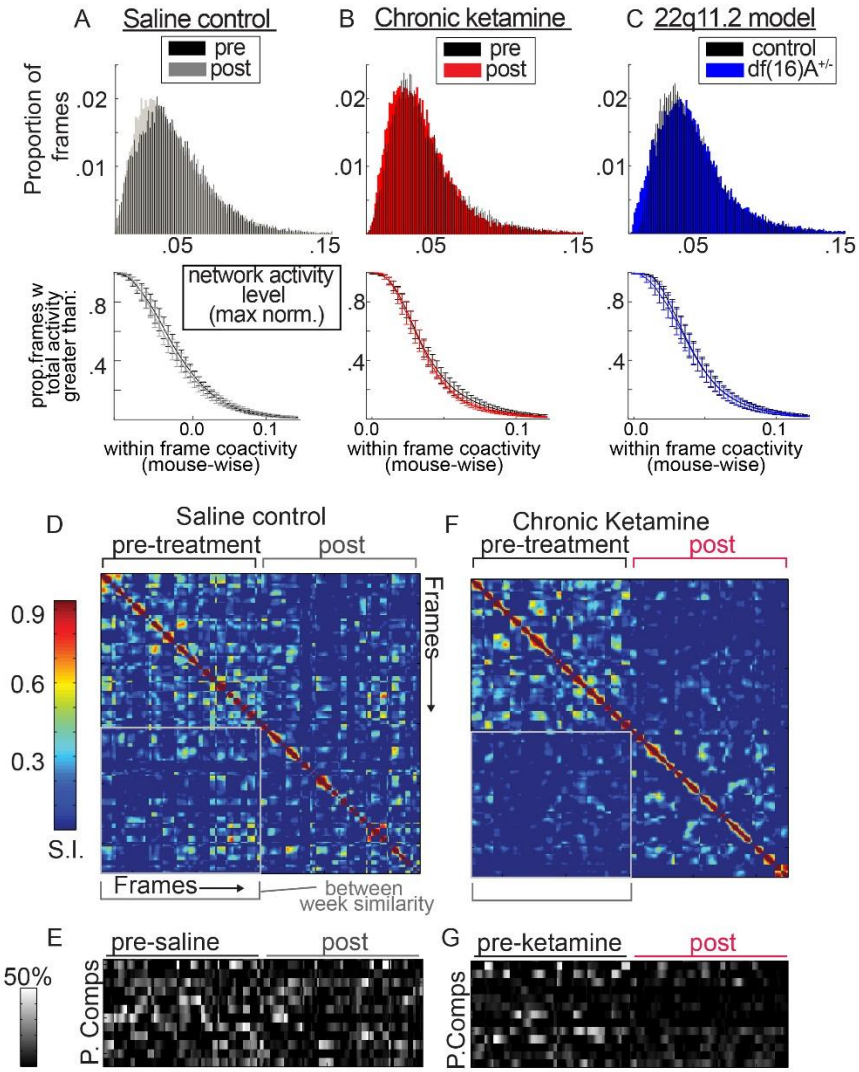

Figure S6. (refers to Figure 4). Network activity levels and upstate stability. (**A-C**) Ensembles activations did not differ in frequency or magnitude between any group or condition**,** as (below) proportion of frames showing "x" amount of activity was nearly identical when averaged across mice. X-axis represents the overall activity present in a given frame as a proportion of maximal activation. (**D**) Matrices of frame-frame similarity values (during ensemble activity), plotted to include within session and between session similarity (highlighted) for 1 representative saline treated and 1 ketamine treated mouse (each with greater than 30 neurons identifiable between weeks). (**E-G**) Twelve principal components extracted from ongoing activity pre-treatment (explaining >70% of the variance) appear after saline but not ketamine. Error bars reflect S.E.M across mice, 6 KET, 6 SAL, 7 Df16, 7 WT.

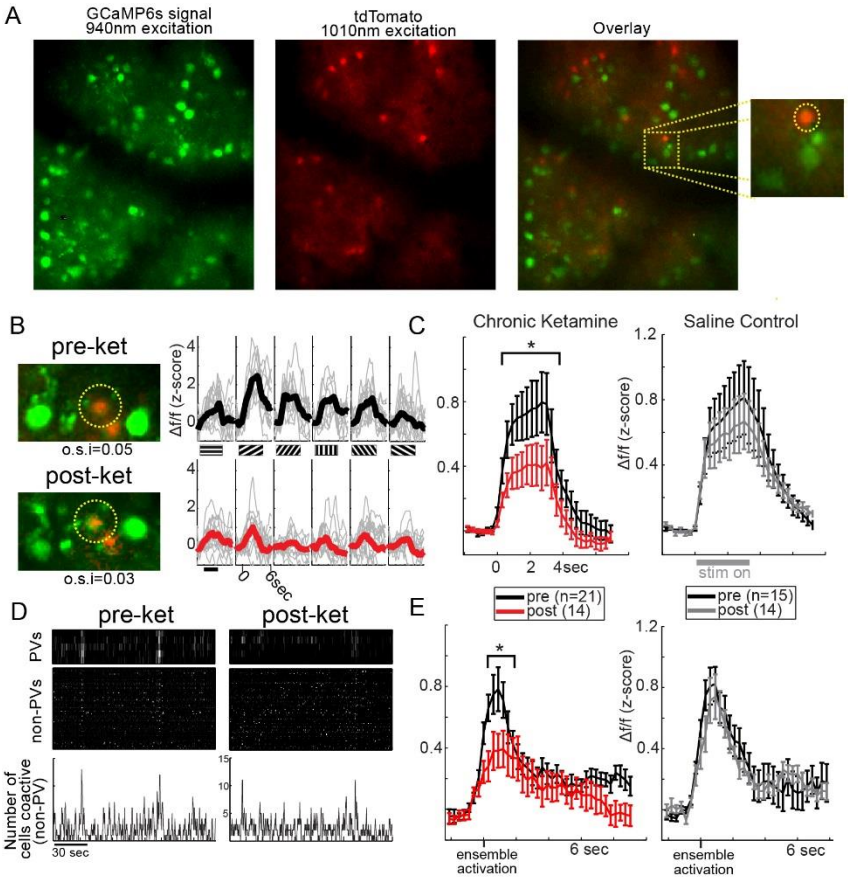

Figure S7. (refers to figure 5). Decreased functional dynamics in parvalbumin-containing interneurons (PVs). Cortex wide anatomical and molecular abnormalities in cortical PVs are well replicated effects seen in post mortem brain tissue of SZ patients (Hashimoto et al., 2008). Here we confirm in our chronic KET model that PVs are also functionally abnormal *in vivo*. (**A**) PVs were identified in a subset of Ai14:LSL:;tdTomato mice by somatic co-localization of GCaMP6s and tdTomato (22 PVs across 3 SAL mice; 34 PVs across 4 KET mice; average of 4 neurons per imaged population), and (**B**) showed clear stimulus driven increases in activity during visual stimulation (but low orientation selectivity, conforming with previously published properties of PVs in (Hofer et al., 2011; Niell and Stryker, 2008)). (**C**) Chronic Ketamine significantly decreased PV activity during stimulation ($F^{interaction}(1,55)=3.88$, $p<.05$; $F^{ket}(1,33)=6.40$, $p<.05$). (**D**) In the absence of visual stimulation, PVs showed activity strongly locked to the onset of ensemble activity in the rest of the network. (**E**) This effect was significantly diminished after chronic ketamine in the initial 2 seconds after the onset of a population "ensemble" activation ($F^{interaction}(1,55)=2.74$, $p<0.1$; $F^{ket}(1,33)=5.34$, $p<.05$). Error bars reflect S.E.M across cells.

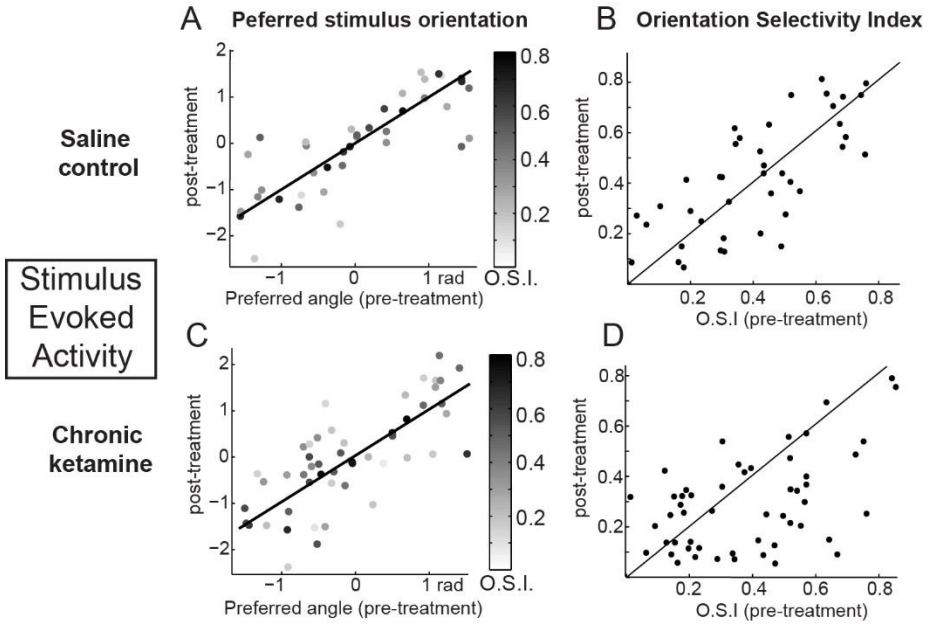

Figure S8 (refers to Figure 6). Stability of visually evoked responses in V1. (**A**) Cells identifiable pre and 1-week post SAL maintained their preferred stimulus orientation and (**B**) quantitative O.S.I. values. (**C**-**D**) cells from 1 week pre and post KET maintained roughly the same preferred stimulus orientation but exhibited a significant decrease in O.S.I. $F(1,97)=8.19$, $p<.01$. ($n^{SAL}=45$ cells, n=4 mice; $n^{KET}=62$, n=5 mice).